



HAL
open science

Identification Of Erythromyeloid Progenitors And Their Progeny In The Mouse Embryo By Flow Cytometry

Lorea Iturri, Javier Saenz Coronilla, Yvan Lallemand, Elisa Gomez Perdiguero

► To cite this version:

Lorea Iturri, Javier Saenz Coronilla, Yvan Lallemand, Elisa Gomez Perdiguero. Identification Of Erythromyeloid Progenitors And Their Progeny In The Mouse Embryo By Flow Cytometry. Journal of visualized experiments : JoVE, 2017, 125, 10.3791/55305 . hal-03263701

HAL Id: hal-03263701

<https://hal.science/hal-03263701>

Submitted on 12 Jul 2021

HAL is a multi-disciplinary open access archive for the deposit and dissemination of scientific research documents, whether they are published or not. The documents may come from teaching and research institutions in France or abroad, or from public or private research centers.

L'archive ouverte pluridisciplinaire **HAL**, est destinée au dépôt et à la diffusion de documents scientifiques de niveau recherche, publiés ou non, émanant des établissements d'enseignement et de recherche français ou étrangers, des laboratoires publics ou privés.

Video Article

Identification Of Erythromyeloid Progenitors And Their Progeny In The Mouse Embryo By Flow Cytometry

Lorea Iturri^{1,2}, Javier Saenz Coronilla¹, Yvan Lallemand¹, Elisa Gomez Perdiguero¹¹Department of Developmental and Stem Cell Biology, CNRS UMR3738, Department of Immunology, Institut Pasteur²Cellule Pasteur UPMC, University Pierre et Marie CurieCorrespondence to: Elisa Gomez Perdiguero at elisa.gomez-perdiguero@pasteur.frURL: <https://www.jove.com/video/55305>DOI: [doi:10.3791/55305](https://doi.org/10.3791/55305)

Keywords: Developmental Biology, Issue 125, Macrophages, yolk sac, definitive hematopoiesis, hematopoietic stem and progenitor cells, mouse embryos, FACS, fate mapping

Date Published: 7/17/2017

Citation: Iturri, L., Saenz Coronilla, J., Lallemand, Y., Gomez Perdiguero, E. Identification Of Erythromyeloid Progenitors And Their Progeny In The Mouse Embryo By Flow Cytometry. *J. Vis. Exp.* (125), e55305, doi:10.3791/55305 (2017).

Abstract

Macrophages are professional phagocytes from the innate arm of the immune system. In steady-state, sessile macrophages are found in adult tissues where they act as front line sentinels of infection and tissue damage. While other immune cells are continuously renewed from hematopoietic stem and progenitor cells (HSPC) located in the bone marrow, a lineage of macrophages, known as resident macrophages, have been shown to be self-maintained in tissues without input from bone marrow HSPCs. This lineage is exemplified by microglia in the brain, Kupffer cells in the liver and Langerhans cells in the epidermis among others. The intestinal and colon lamina propria are the only adult tissues devoid of HSPC-independent resident macrophages. Recent investigations have identified that resident macrophages originate from the extra-embryonic yolk sac hematopoiesis from progenitor(s) distinct from fetal hematopoietic stem cells (HSC). Among yolk sac definitive hematopoiesis, erythromyeloid progenitors (EMP) give rise both to erythroid and myeloid cells, in particular resident macrophages. EMP are only generated within the yolk sac between E8.5 and E10.5 days of development and they migrate to the fetal liver as early as circulation is connected, where they expand and differentiate until at least E16.5. Their progeny includes erythrocytes, macrophages, neutrophils and mast cells but only EMP-derived macrophages persist until adulthood in tissues. The transient nature of EMP emergence and the temporal overlap with HSC generation renders the analysis of these progenitors difficult. We have established a tamoxifen-inducible fate mapping protocol based on expression of the macrophage cytokine receptor *Csf1r* promoter to characterize EMP and EMP-derived cells *in vivo* by flow cytometry.

Video Link

The video component of this article can be found at <https://www.jove.com/video/55305/>

Introduction

There are several successive but overlapping waves of hematopoietic progenitors during development whose myeloid progeny remain into adulthood. First, unipotent "primitive" progenitors emerge in the mouse yolk sac^{1,2} between E7.5-E8.25 and give rise to embryonic macrophages without any monocytic intermediate. Whether macrophages derived from primitive progenitors persist in the adult brain as microglia remains a subject of active investigation. Second, Erythro-Myeloid Precursors (EMPs) arise in the yolk sac at E8.5, enter the bloodstream and colonize the embryo. EMPs emerge from the yolk sac hemogenic endothelium in a *Runx1*-dependant endothelial-to-hematopoietic transition^{3,4}. While EMP can differentiate into macrophages within the yolk sac, they also colonize the fetal liver from embryonic day (E)9⁵ and differentiate into erythrocytes, megakaryocytes, macrophages, monocytes granulocytes and mast cells⁶. The macrophages that derive from EMPs exhibit proliferative capacity in developmental and adult tissues. Whether EMP-derived macrophages bypass the monocyte stage of differentiation is still controversial as very little is known about their differentiation pathway^{7,8}. Finally, Hematopoietic Stem Cells (HSCs) emerge at E10.5 within the embryo proper from the aorta-gonad-mesonephros region and migrate to the fetal liver. HSCs with long-term repopulation capacity are only detected after E11 (at the 42 somite pair stage)⁹. There, they expand and differentiate from E12.5 until definitive hematopoiesis begins to shift to the bone marrow, which becomes the predominant site of blood cell production for the duration of postnatal life¹⁰.

The spatial and temporal overlap in emergence, as well as shared immuno-phenotypic markers has thus far hampered our ability to distinguish the specific contributions of these waves of embryonic hematopoietic progenitors. While both EMP and HSC are generated in a *Runx1*-dependent manner and express the transcription factor *Myb* and the growth factor receptor *Csf1r* (Colony-Stimulating Factor 1 Receptor, also known as Macrophage Colony Stimulating Factor Receptor) among others, EMPs can be distinguished from HSCs by their lack of lymphoid potential, both *in vitro* and *in vivo*, their lack of long-term repopulating potential and lack of surface expression of the lineage marker *Sca-1*¹¹. Genetic fate mapping models are required to characterize macrophage ontogeny since they allow targeting embryonic progenitors in a cell-specific and time-specific manner. Here we present the fate-mapping protocol used in our laboratory to discriminate between the two lineages of macrophages found in most adult tissues: HSC-derived infiltrating macrophages and HSC-independent resident macrophages.

Tissue resident macrophages have been traced back to *Myb*-independent precursor cells expressing the cytokine receptor *Csf1r*¹² and are present in the embryo at E8.5-E10.5 using three complementary fate-mapping strategies⁶. In order to study yolk sac hematopoiesis without

labeling fetal HSCs, we use a transgenic strain, *Csf1r*^{MeriCreMer}, expressing a tamoxifen-inducible fusion protein of 'improved' Cre recombinase and two mouse estrogen receptors (Mer-iCre-Mer) under the control of the *Csf1r* promoter. Hence, the Cre recombinase will be active in *Csf1r*-expressing cells during a limited time-window. When used with a reporter strain containing a fluorescent protein downstream of a lox-STOP-lox cassette (*Rosa26*^{LSL-eYFP}), it will lead to the permanent genetic labeling of the cells present at the time of induction but also of their progeny. Administration at E8.5 of the active form of tamoxifen, 4-hydroxytamoxifen (OH-TAM), labels EMPs and macrophages, without labeling yolk sac unipotent "primitive" progenitors or fetal HSCs. Thereby, we have characterized the immunophenotype of EMPs and their progeny during embryonic development, as well as assessed the contribution of yolk sac-derived macrophages to the adult macrophage pools. Further work is required to characterize whether primitive progenitor-derived macrophages are also labeled using this approach and whether they can contribute to adult macrophage pools.

Protocol

Animal procedures were performed in accordance with the approved institutional animal care and use committee of the Institut Pasteur (CETEA).

1. *In Utero* Pulse Labeling in *Csf1r*^{MeriCreMer} *Rosa*^{LSL-YFP} Embryos

1. Prepare the stock solution of 4-hydroxytamoxifen (OH-TAM, 50 mg/mL).

1. Under the fumehood, open the 25 mg vial of OH-TAM and add 250 μ L ethanol (100%).
2. Transfer the OH-TAM solution to a 2 mL microcentrifuge tube with a truncated tip and vortex at maximum speed for 10 min.
3. Sonicate 30 min in a sonicator bath.
4. Add 250 μ L of PEG-35 castor oil under the fumehood to obtain a 50 mg/mL stock solution.
NOTE: PEG-35 castor oil is a solvent with amphiphilic properties that binds hydrophobic molecules and solubilizes them in aqueous solvents.
5. Vortex for approximately 5 min at maximum speed and sonicate 30 min in a sonicator bath.
6. Aliquot 90 μ L (4.5 mg) per microcentrifuge tube (1 aliquot per injection).
7. Store at 4 °C for 1 week or at -20 °C for long term as previously described¹³.

2. Prepare the stock solution of Progesterone (10 mg/mL)

1. Add 250 μ L of 100% Ethanol to 25 mg of progesterone to prepare a 10 mg/100 μ L suspension under the fumehood. Vortex gently.
2. Add 2250 μ L autoclaved sunflower oil to make 10 mg/ml progesterone solution under the hood.
3. Vortex for approximately 5 min at maximum speed, aliquot and store at 4 °C. Note that the solution is clear when stored.

3. Tamoxifen administration

NOTE: Embryonic development was estimated considering the day of vaginal plug formation as Embryonic day (E) 0.5. Recombination is induced by single injection at E8.5 into pregnant *Csf1r*^{MeriCreMer} females¹². Supplement OH-TAM with 37.5 μ g per g of Progesterone to reduce abortion rates after tamoxifen administration. Inject at 1 pm (for vaginal plug observed in the morning).

1. On the morning of injection, sonicate an aliquot of the OH-TAM solution for 10 min (or until completely resuspended).
2. Add 360 μ L NaCl 0.9% under the fumehood to obtain a 10 mg/mL OH-TAM solution and vortex thoroughly. Sonicate until the solution is clear and completely resuspended (at least 30 min).
3. Pre-warm progesterone to room temperature.
4. Mix 450 μ L of OH-TAM and 225 μ L of progesterone in a microcentrifuge tube. Vortex.
5. Sonicate at least 10 min and load on to a 1 mL syringe with a 25G needle.
6. In the animal facility, weigh the pregnant female (*Csf1r*^{MeriCreMer} females are in an inbred FVB genetic background and typical weigh between 25 and 33 g).
7. Perform an intra-peritoneal injection by slowly injecting the calculated volume into the mouse. After withdrawing the needle, gently press on the puncture wound and massage the abdomen to distribute the OH-TAM.

NOTE: The OH-TAM injection dose is 75 mg/kg and the Progesterone dose is 37.5 mg/kg. **Table 1** provides the volume to inject into pregnant females.

Mouse weight (g)	Total volume to inject from the mix (μL)
25	281
26	292
27	303
28	315
29	326
30	338
31	348
32	360
33	371
34	382
35	394

Table 1: Injection volume of 4-OH-tamoxifen (OH-TAM). Volume required for a single injection at E8.5 of 75 μg per g (body weight) of OH-TAM supplemented with 37.5 μg per g of progesterone.

2. Dissection of the Yolk Sac (YS) and Fetal Liver (FL)

NOTE: Rigorous sterile techniques are not necessary when manipulating embryos unless if they are going to be used for long-term culture. Nevertheless, the working area must be clean and covered in foil under absorbent paper.

1. Prepare ice-cold phosphate buffered saline (PBS) and digestion mix (PBS containing 1 mg/mL collagenase D, 100 U/mL Deoxyribonuclease I (DNase I) and 3% fetal bovine serum).
2. Sacrifice pregnant females by cervical dislocation at the required gestation day (e.g. embryonic stage E10.5).
3. Pinch the skin just over the genitals and make a small incision at the midline with scissors. Pull the skin toward the head to expose completely the body wall without fur. Cut the abdominal muscles to expose the internal organs and push the gut to expose the two uterine horns.
4. With middle-sized blunt forceps, grab the fat-pad attached to the ovary and gently pull the uterus. Cut at the cervical level of the uterine horns and lift the horns from the peritoneal cavity. Remove the fat-pad to completely free the uterine horns and cut the horns from the ovary on each side.
5. Put the horns into ice-cold PBS in a 10 mm Petri dish. Rapidly grip the uterus muscle layers at one extremity (cervical end) and slide fine scissors between the muscle layer and the decidual tissue to release the embryos with the surrounding decidual tissue.
NOTE: Muscle tend to rapidly contract after the extraction, so this step must be as quick as possible.
6. Use one pair of fine forceps to cut off the Reichert's membrane and the placenta.
7. **Gently remove the yolk sac and place it in a 24-well tissue culture plate with 0.5 mL of digestion mix.**
NOTE: At this step, embryonic blood can be collected.
 1. Immediately after severing the umbilical and vitelline vessels, transfer the embryo into a 12-well tissue culture plate containing 10 mM ice-cold ethylenediaminetetraacetic acid (EDTA). Decapitate the embryo using sharp fine scissors, trying to limit as much as possible tissue dilaceration. Incubate on ice for 10-15 min and collect the EDTA containing the blood.
8. Remove the amnion surrounding the embryo.
9. For stages <E11.5, count the number of somite pairs for better staging of embryos and a better time resolution (each somite pair develops in ~1 h 30 min).
10. Cut the head of the embryo using forceps or fine scissors. Transfer the head to a 24-well plate with 0.5 mL digestion mix.
NOTE: The neuroectoderm and brain at later stages are further dissected for flow cytometry analysis; carefully remove the surrounding vascular plexus.
11. Cut the embryo above the hindlimb and remove the forelimbs.
12. **To isolate the liver, open the thorax using a pair of fine forceps. Pinch anteriorly to the heart and gently pull while using the second forceps to free the organs from the body.**
 1. Carefully separate the fetal liver from the heart and gut. Transfer the fetal liver to a 24-well plate with 0.5 mL digestion mix. Carefully monitor the transfer under the dissecting microscope.
13. Collect the tail region (or any other embryo part) for genotyping by polymerase chain reaction assay (PCR).
NOTE: Other tissues and organs can be harvested from E10.5 embryos for a similar analysis using flow cytometry. Blood, head skin, aorta-gonad-mesonephros region (AGM), heart and neuroectoderm can be collected at E10.5. At later stages, lung, kidney, spleen and pancreas can also be collected. A detailed description of the dissection of the AGM at different developmental stages has been previously described¹⁴.

3. Processing of Embryonic Tissues for Flow Cytometry

1. Incubate the organs (placed in the digestion mix) for 30 min at 37 °C.
2. Transfer the tissue and enzymatic solution onto a 100 μm strainer placed in a 6-well tissue culture plate filled with 6 ml of FACS buffer (0.5% Bovine Serum Albumin (BSA) and 2 mM EDTA in 1x PBS). Mechanically dissociate by gently mashing with the black rubber piston of a 2 mL syringe to obtain a single-cell suspension.

NOTE: From now on, all steps should be performed at 4 °C.

3. Collect the cell suspension with a Pasteur pipette and transfer into a 15 mL tube.
4. Spin for 7 min at 320 x g at 4 °C. Discard the supernatant by aspiration.
5. **Resuspend the pellet in 60 µL Fc-blocking buffer (CD16/CD32 blocking antibody diluted 1/50 in FACS buffer).**
 1. Transfer 50 µL of the single-cell suspension per well in a round bottom 96 multi-well plate. Incubate for at least 15 min on ice.
NOTE: The staining can also be performed in 5 mL polystyrene FACS tubes when handling a small number of samples.
 2. Transfer the remaining 10 µL into a 5 mL polystyrene FACS tube to obtain a pool of the samples from each tissue. This pool will serve as the controls (*i.e.* unstained samples and fluorescent minus one (FMO) controls for each fluorochrome). Transfer 50 µL of the pool for each fluorescent minus one (FMO) control (one per fluorochrome) to the 96 multi-well plate.
NOTE: Each FMO control contains all the fluorochrome-coupled antibodies from the antibody panel, except for the one that is being measured. FMOs are used to identify gate boundaries and to control for the spectral overlap in multicolor panels. To correctly address the variations in background and autofluorescence between different tissues, it is important to prepare these controls from the pool of samples of each tissue. The appropriate control for YFP expression will be the samples from Cre-negative embryos, which are confirmed by PCR genotyping.

4. Surface Antigen Staining

1. **Prepare the antibody mix in FACS buffer (Table 2). Prepare 50 µL of antibody mix per sample.**
 1. Use the following fluorochrome-coupled antibodies: anti-CD45.2 (clone 104); anti-CD11b (clone M1/70); anti-F4/80 (clone BM8); anti-AA4.1 (clone AA4.1); anti-Kit (clone 2B8); and anti-Ter119 (clone Ter119).
 2. Prepare six antibody mixes for the FMO controls in FACS buffer. Prepare 50 µL of antibody mix per control sample.
NOTE: The antibody dilution in the antibody mix is two times more concentrated than the final concentration indicated in the materials table. For a panel with six fluorochrome-coupled antibodies, 6 FMO controls are prepared. **Table 2** provides the composition of the antibody mix and FMO controls for one tube.

Antibody	Clone	Volume (µL) of antibody (Final Volume 50 µL)						
		Antibody Mix	FMO CD45.2	FMO CD11b	FMO F4/80	FMO AA4.1	FMO Kit	FMO Ter119
anti-CD45.2	104	1	0	1	1	1	1	1
anti-CD11b	M1/70	0.5	0.5	0	0.5	0.5	0.5	0.5
anti-F4/80	BM8	1	1	1	0	1	1	1
anti-AA4.1	AA4.1	1	1	1	1	0	1	1
anti-Kit	2B8	0.5	0.5	0.5	0.5	0.5	0	0.5
anti-Ter119	Ter119	0.5	0.5	0.5	0.5	0.5	0.5	0
FACS buffer		45.5	46.5	46	46.5	46.5	46	46

Table 2: Volume of antibodies using for staining and Fluorescent minus one (FMO) controls. Volume (µL) of antibody required for a final volume of 50 µL.

2. Add 50 µL of the antibody mix to the samples in the 96-multiwell plate (final volume during staining is 100 µL). Gently pipette up and down twice and incubate on ice for 30 min.
3. Spin the 96-multiwell plate for 7 min at 320 x g at 4 °C and discard the supernatant. Resuspend in 200 µL of FACS buffer.
4. Repeat wash procedure (step 4.3) twice with 150 µL FACS buffer.
5. Filter the samples and the controls (FMOs and unstained pool samples) into 5 ml polystyrene tubes through a 70 µm strainer. Store on ice until acquisition.

5. Identification of EMPs and YS-derived Macrophages by Flow Cytometry

NOTE: This protocol was optimized using a 4 laser flow cytometer equipped with a 405 nm Violet laser, a 488 nm Blue laser, a 562 nm Yellow laser and a 638 nm Red laser.

1. Prepare compensation beads for each coupled antibody following the manufacturer's instructions. Use unstained samples and compensation beads to optimize laser intensities.
2. To identify gate boundaries, use FMO (Fluorescence minus one) controls for each antibody.
3. In order to exclude dead cells, add 1 µL of DAPI (1 mg/ml) to the tube (containing 200 µL of stained cell suspension) 1 min before acquisition. Use the strong DAPI signal and the forward-scattered parameter (FSC) to perform exclusion of dead cells and debris.
NOTE: Use software from the flow cytometer to draw gates during acquisition. Compensation matrix and analysis can be performed after sample acquisition using other commercially available software.
4. Use forward and side scatter (FSC vs SSC) to perform live cell and doublet discrimination from total events.
5. Create fluorescence dot plots in log-scale axis and draw daughter gates to, first, exclude erythrocytes (Ter119⁺) and, then, to identify progenitor cells (Kit⁺) and hematopoietic cells (CD45⁺ Kit^{neg}) (See **Figure 1**).
6. Create fluorescence histograms to quantify the labeling efficiency of YFP among the different identified populations in the YS (**Figure 2**), fetal liver (**Figure 3**) and brain (**Figure 4**).

Representative Results

Genetic fate mapping was achieved by administration at E8.5 of OH-TAM into *Csf1r*-Mer-iCre-Mer females mated with males carrying a *Rosa26*-LSL-eYFP reporter. In the presence of OH-TAM, excision of the stop cassette leads to the permanent expression of YFP in the cells expressing *Csf1r*. We collected two hematopoietic tissues: the yolk sac and the fetal liver and a non-hematopoietic tissue, the neuroectoderm, from the embryos at E10.5. Single-cell suspensions were obtained by enzymatical and mechanical dissociation and samples were analyzed by flow cytometry after staining with fluorescent-coupled antibodies. After exclusion of dead cells and doublets, single cell suspensions were analyzed (Figure 1). All gates were defined using Fluorescence Minus One (FMO) controls. It is recommended to also perform an erythrocyte exclusion (Ter119^+ cells) to improve clarity of the analysis (Figure 1B). Using the cell surface markers *Kit* (progenitor marker) and *CD45* (hematopoietic cells marker), we were able to distinguish three populations of cells of interest: $\text{Kit}^+ \text{CD45}^{\text{neg}}$, $\text{Kit}^+ \text{CD45}^{\text{low}}$ and $\text{Kit}^{\text{neg}} \text{CD45}^+$ (Figure 1). Progenitors were further analyzed based on their expression of AA4.1 (Figures 2-4). Indeed, AA4.1 is a surface marker that allows the enrichment of the progenitor population within erythromyeloid progenitors in the yolk sac, as demonstrated in colony forming assays¹⁵. Once the populations of interest were identified, we quantified the YFP labeling efficiency in each population using histograms. Among the yolk sac Kit^+ progenitors, both CD45^{neg} (Figure 2A) and CD45^{low} (Figure 2B) cell populations contain AA4.1⁺ YFP⁺ cells. However, AA4.1⁺ YFP⁺ cells in the liver and brain are only found in the $\text{Kit}^+ \text{CD45}^{\text{low}}$ progenitor population (Figure 3B and 4B). Since, the brain is not an active site of hematopoiesis, progenitors found in this tissue could correspond to circulating progenitors. This also suggests a process of progenitor maturation as they migrate from the yolk sac to the fetal liver and the peripheral tissues. Kit^+ progenitors first express AA4.1, irrespectively of *CD45* expression, but by the time they reach circulation and the fetal liver, all AA4.1⁺ YFP⁺ progenitors express detectable levels of cell surface *CD45*. Macrophages, defined as $\text{F4/80}^{\text{bright}} \text{CD11b}^+$, were found in the $\text{Kit}^{\text{neg}} \text{CD45}^+$ gate (Figure 2-4). Macrophages in the E10.5 yolk sac, liver and brain were efficiently labeled (60 to 80% of $\text{F4/80}^{\text{bright}} \text{CD11b}^+$ cells are YFP⁺) by a single OH-TAM administration at E8.5 (Figure 2C, 3C and 4C).

To compare labeling efficiency between litters, we recommend that an internal control for recombination efficiency is used. Variability in the level of expression of the reporter can be observed between experiments, due to variations in developmental timing between litters and mouse strains when OH-TAM is injected *in utero*. Hence, we recommend that embryo staging from E8.5 to E11.5 embryos is performed by somite pair counting. In this protocol, we propose to use the labeling efficiency in the brain resident macrophages (microglia) as a reference to compare the efficiency of Cre recombination between different experiments and strains (Figure 4C). Other resident macrophages could be used, however microglia were the first cells to be described as yolk sac-derived macrophages¹⁶ and they represent the most abundant population of tissue resident macrophages at E10.5. Thus, YFP labeling in microglia can be used to assess the fate-mapping efficiency in each experiment and compare data from different litters.

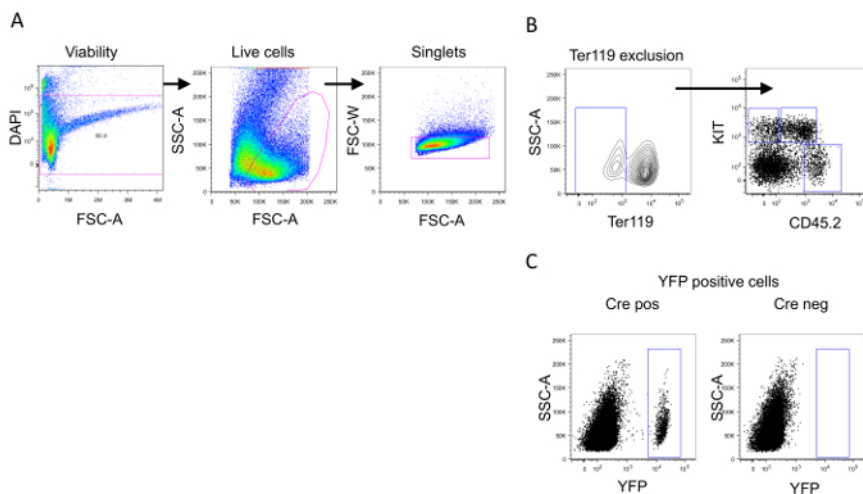


Figure 1: Gating strategy to identify progenitor cells ($\text{Kit}^+ \text{CD45}^{\text{neg}}$ and $\text{Kit}^+ \text{CD45}^{\text{low}}$) and differentiated hematopoietic cells ($\text{Kit}^{\text{neg}} \text{CD45}^+$). (A) Discrimination of live cells and singlets is performed using DAPI staining and Forward and Side scatter (FSC/SSC) parameters. (B) Following red blood cell exclusion ($\text{Ter119}^{\text{neg}}$), three populations of cells of interest are identified based on cell surface expression of *Kit* and *CD45*: $\text{Kit}^+ \text{CD45}^{\text{neg}}$, $\text{Kit}^+ \text{CD45}^{\text{low}}$ and $\text{Kit}^{\text{neg}} \text{CD45}^+$ cells. (C) *Csf1r*-expressing cells present when OH-TAM is injected and their progeny are identified in Cre-recombinase positive embryos as expressing YFP compared to the Cre-recombinase negative embryos (confirmed later by polymerase chain reaction assay, PCR). [Please click here to view a larger version of this figure.](#)

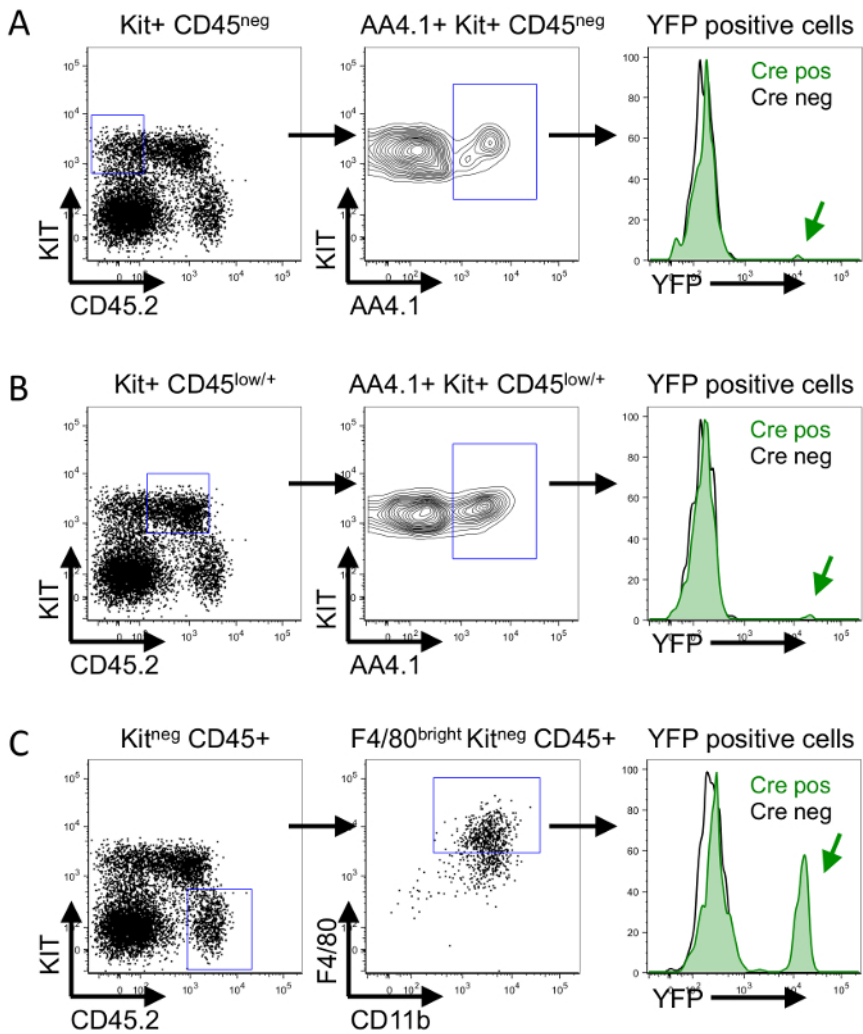


Figure 2: Labeling efficiency in the yolk sac from E10.5 $Csf1r^{MerCreMer}$ $Rosa26^{LSL-eYFP}$ embryospulsed with OH-TAM at E8.5. (A) $Kit^+ CD45^{neg}$ cells are gated based on Kit and CD45 expression on live yolk sac cells (blue gate, left panel). AA4.1 and Kit expression on $Kit^+ CD45^{neg}$ cells. Blue gate encloses AA4.1 $^+ Kit^+ CD45^{neg}$ cells (middle panel). Comparison of YFP labeling in AA4.1 $^+ Kit^+ CD45^{neg}$ cells (right panel) in Cre negative controls (black) and Cre positive samples (green). Histograms represent the percentage of cells (y-axis) positive for YFP signal (x-axis). **(B)** $Kit^+ CD45^{low/+}$ cells are gated based on Kit and CD45 expression (blue gate, left panel). AA4.1 and Kit expression on $Kit^+ CD45^{low/+}$ cells. Blue gate encloses EMP, as defined as AA4.1 $^+ Kit^+ CD45^{low/+}$ cells (middle panel). Comparison of YFP labeling in AA4.1 $^+ Kit^+ CD45^{low/+}$ cells (right panel) in Cre negative controls (black) and Cre positive samples (green). Histograms represent the percentage of cells (y-axis) positive for YFP signal (x-axis). **(C)** Hematopoietic cells are defined as $Kit^{neg} CD45^+$ and gated in blue (left panel). F4/80 and CD11b expression on $Kit^{neg} CD45^+$ cells. Macrophages are defined as F4/80 $^{bright} CD11b^+$ cells (middle panel). Comparison of YFP labeling in F4/80 $^{bright} CD11b^+$ macrophages (right panel) in Cre negative controls (black) and Cre positive samples (green). Histograms represent the percentage of cells (y-axis) positive for YFP signal (x-axis). [Please click here to view a larger version of this figure.](#)

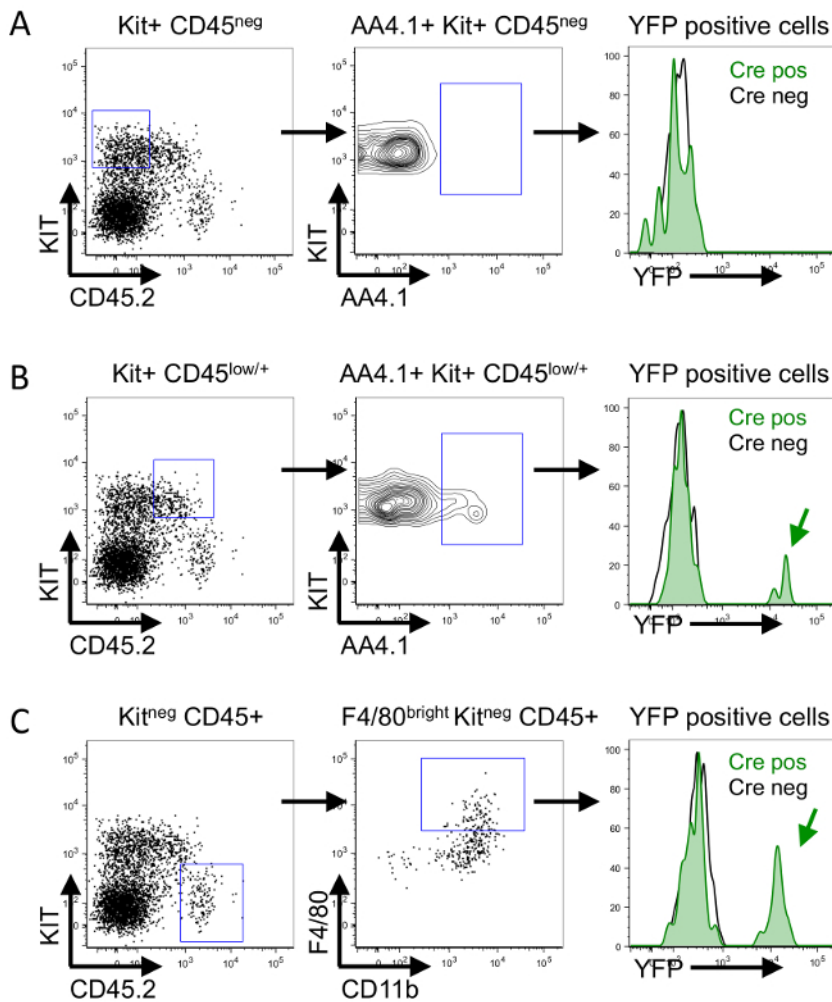


Figure 3: Labeling efficiency in the liver from E10.5 $Csf1^{MeriCreMer} Rosa26^{LSL-eYFP}$ embryos pulsed with OH-TAM at E8.5. (A) $Kit^+ CD45^{neg}$ cells are gated based on Kit and CD45 expression on live liver cells (blue gate, left panel). AA4.1 and Kit expression on $Kit^+ CD45^{neg}$ cells. Blue gate encloses AA4.1⁺ $Kit^+ CD45^{neg}$ cells (middle panel). Comparison of YFP labeling in AA4.1⁺ $Kit^+ CD45^{neg}$ cells (right panel) in Cre negative controls (black) and Cre positive samples (green). Histograms represent the percentage of cells (y-axis) positive for YFP signal (x-axis). (B) $Kit^+ CD45^{low/+}$ cells are gated based on Kit and CD45 expression (blue gate, left panel). AA4.1 and Kit expression on $Kit^+ CD45^{low/+}$ cells. Blue gate encloses EMP, as defined as AA4.1⁺ $Kit^+ CD45^{low/+}$ cells (middle panel). Comparison of YFP labeling in AA4.1⁺ $Kit^+ CD45^{low/+}$ cells (right panel) in Cre negative controls (black) and Cre positive samples (green). Histograms represent the percentage of cells (y-axis) positive for YFP signal (x-axis). (C) Hematopoietic cells are defined as $Kit^{neg} CD45^+$ and gated in blue (left panel). F4/80 and CD11b expression on $Kit^{neg} CD45^+$ cells. Macrophages are defined as F4/80^{bright} CD11b⁺ cells (middle panel). Comparison of YFP labeling in F4/80^{bright} CD11b⁺ macrophages (right panel) in Cre negative controls (black) and Cre positive samples (green). Histograms represent the percentage of cells (y-axis) positive for YFP signal (x-axis). [Please click here to view a larger version of this figure.](#)

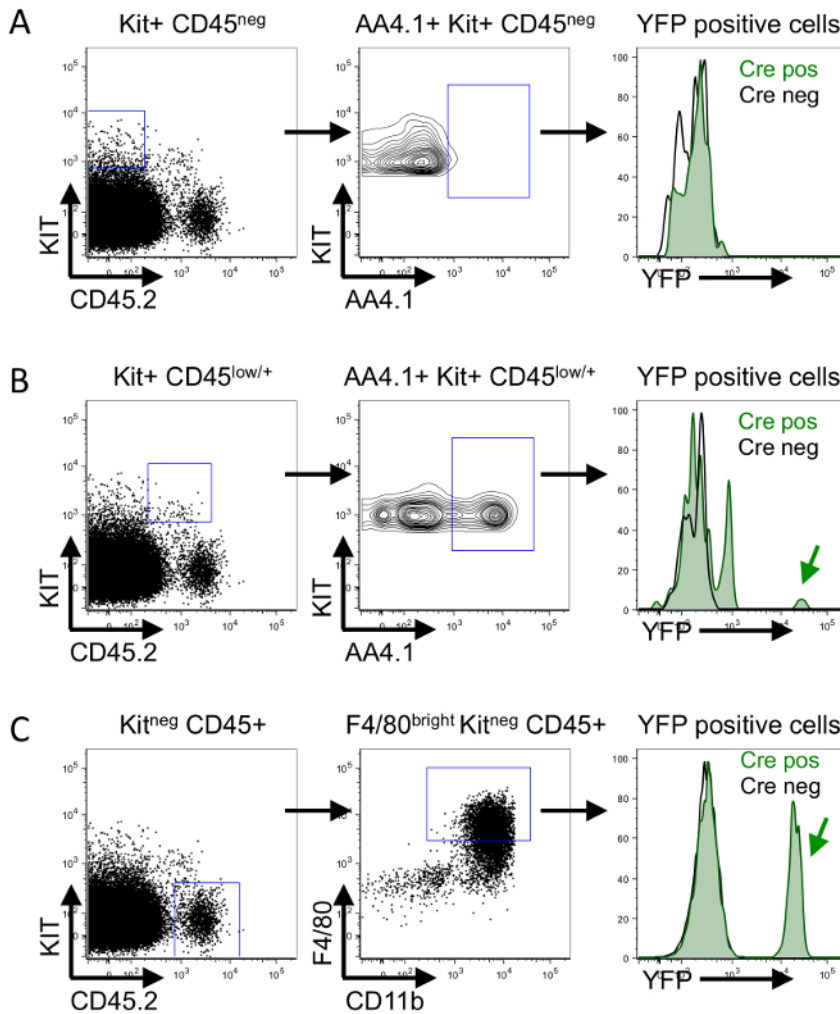


Figure 4: Labeling efficiency in the brain from E10.5 $Csf1^{MerCreMer}$ $Rosa26^{LSL-eYFP}$ embryospulsed with OH-TAM at E8.5. (A) $Kit^+ CD45^{neg}$ cells are gated based on Kit and CD45 expression on live brain cells (blue gate, left panel). AA4.1 and Kit expression on $Kit^+ CD45^{neg}$ cells. Blue gate encloses AA4.1⁺ $Kit^+ CD45^{neg}$ cells (middle panel). Comparison of YFP labeling in AA4.1⁺ $Kit^+ CD45^{neg}$ cells (right panel) in Cre negative controls (black) and Cre positive samples (green). Histograms represent the percentage of cells (y-axis) positive for YFP signal (x-axis). **(B)** $Kit^+ CD45^{low/+}$ cells are gated based on Kit and CD45 expression (blue gate, left panel). AA4.1 and Kit expression on $Kit^+ CD45^{low/+}$ cells. Blue gate encloses EMP, as defined as AA4.1⁺ $Kit^+ CD45^{low/+}$ cells (middle panel). Comparison of YFP labeling in AA4.1⁺ $Kit^+ CD45^{low/+}$ cells (right panel) in Cre negative controls (black) and Cre positive samples (green). Histograms represent the percentage of cells (y-axis) positive for YFP signal (x-axis). **(C)** Hematopoietic cells are defined as $Kit^{neg} CD45^+$ and gated in blue (left panel). F4/80 and CD11b expression on $Kit^{neg} CD45^+$ cells. Macrophages are defined as F4/80^{bright} CD11b⁺ cells (middle panel). Comparison of YFP labeling in F4/80^{bright} CD11b⁺ macrophages (right panel) in Cre negative controls (black) and Cre positive samples (green). Histograms represent the percentage of cells (y-axis) positive for YFP signal (x-axis). [Please click here to view a larger version of this figure.](#)

Discussion

The different waves of hematopoietic precursor cells partially overlap within a short time frame, which makes the analysis of the contribution of each wave of developmental hematopoiesis to immune cells technically very challenging.

Tamoxifen-inducible Cre systems offer the opportunity to tag specific cells in a temporally inducible manner and to perform lineage analysis in embryos or adults, without the need for *ex vivo* or *in vitro* culture or transplantation. In tamoxifen-inducible Cre strains, a fusion gene is created between a bacterial Cre recombinase and a mutant form of the ligand binding domain of the human estrogen receptor (CRE-ER) or between an improved single-point mutant Cre and two mouse estrogen receptors (Mer-iCre-Mer). Fusion of Cre with estrogen receptors leads to the cytoplasmic sequestration of Cre by Hsp90, thereby preventing nuclear Cre-mediated recombination. Tamoxifen (TAM) is metabolized by the liver into 4-hydroxytamoxifen (OH-TAM), its active metabolite with high binding affinity for estrogen receptor. OH-TAM binding to the fusion Cre leads to the disruption of the interaction with Hsp90, permitting its translocation to the nucleus and initiation of Cre-mediated recombination. Injection of TAM or OH-TAM *in utero* into pregnant females has been shown to activate recombination in the developing embryo. Tamoxifen administration during pregnancy can lead to abortion and thus reduces litter size but it also prevents birth if delivered after mid-gestation, in

which case pup delivery through a caesarean operation is required. To counterbalance tamoxifen effects during pregnancy, we supplement OH-TAM administration with a half-dose of progesterone, in order to improve survival of embryos and reduce the risk of abortions¹⁷.

Several routes can be employed to deliver TAM or OH-TAM into pregnant females. Currently oral gavage or intra peritoneal (ip) injection is used for tamoxifen. OH-TAM has the advantage to be immediately available, as it does not require to be metabolized by the liver of the pregnant dam. However, while tamoxifen is very easy to dissolve in corn oil, OH-TAM is very difficult to prepare using the same technique and results in an emulsion. This has been a limiting step in employing OH-TAM for *in utero* pulse labeling. We have adapted the protocol for preparation of OH-TAM developed by the group of J.F. Nicolas¹³, where they use PEG-35 castor oil, a solvent with amphiphilic properties to solubilize OH-TAM, as tamoxifen dissolution is one of the most critical steps in the procedure. This allows for reproducible and optimal preparation of OH-TAM and considerably shortens the time of tamoxifen preparation. Further, it is necessary to adapt the concentration of OH-TAM to inject when using different inducible Cre strains. The combination of a viability dye (DAPI) and size (FSC) is critical to remove dead cells and cellular debris, respectively. Dead cells and debris are highly autofluorescent in most of the violet, blue and red laser detectors, and can hamper flow cytometric analysis. Further, we do not recommend fixing the cells after staining prior to analysis with the flow cytometer. Fixation can lead to changes in cell morphology and thus renders difficult size discrimination based on Forward and Side Scatter (FSC vs. SSC). Further, fixation of samples with PFA leads to a significant loss of YFP fluorescent intensity.

The main limitation within this protocol is that the populations are not tested on their functionality and differentiation potential. In order to overcome this, cells can be sorted following a similar protocol using a Fluorescently-activated cell sorter (FACS) to perform colony-forming assay. In this case, the procedure must be performed under sterile conditions and use of fetal bovine serum (FBS) in the FACS buffer, instead of BSA, is highly recommended. The low labeling efficiency achieved with this technique and the consequently low number of YFP⁺ cells of interest per embryonic tissue is a major challenge in the study of EMP phenotype. This protocol uses a 4-laser flow cytometer. A flow cytometer with 3 lasers can also be used but it is important to adapt the antibody panel to take into account the increased spectral overlap between dyes. Additionally, titration of antibodies is required to find the appropriate concentration when changing the antibody panel and we recommend performing titration of antibodies and validation of the new antibody panel in a pilot experiment where all embryos per tissue are pooled, in order to increase the number of cells analyzed per tissue.

The field of developmental biology has been revolutionized by the Cre/Lox method, which allows permanent labeling of cells *in situ*. This approach achieves tissue- or cell type -specificity through expression of the Cre recombinase under the control of a specific promoter. In our case, we chose to study the expression of the Cre recombinase under the control of the promoter of Csf1r (Colony Stimulating Factor 1 Receptor), an important mitogenic and growth factor receptor for macrophages and their progenitors, using a strain developed by the group of J. Pollard¹⁸. The advantage of a fate mapping strategy based on Csf1r expression compared to other published strategies is that it allows the labeling of yolk sac-derived cells (EMP and macrophages) without labeling any fetal HSCs¹². The Cx3cr1^{CreERT2} strain can also label yolk sac cells without labeling HSCs¹⁹, however it can only label macrophages and macrophage precursors but it does not label EMP progenitors¹. The Cx3cr1^{CreERT2} strain has the same caveat as the Csf1r^{MerCreMer} line, since it cannot distinguish between macrophages derived from unipotent primitive macrophage progenitors or from EMP. When tamoxifen is administered as early as E7.5 in both Runx1^{MerCreMer16} and Kit^{MerCreMer20}, peripheral blood cells are always labeled in adults, albeit at a very low efficiency, thus demonstrating labeling of HSCs during development. Further, Kit^{MerCreMer} fate mapping labels yolk sac Kit⁺ Sca1⁺ progenitors while EMP are Kit⁺ Sca1⁻ negative¹¹. The Csf1r^{MerCreMer} strain is not a knock-in but it was generated by classical additive transgenesis, thus expression of the Cre may not fully recapitulate endogenous expression of Csf1r. However, this has the advantage to avoid any potential developmental defects due heterozygous expression of Csf1r. This is an important factor to take to account when analyzing other fate mapping strategies used for developmental hematopoiesis studies, such as Runx1^{MerCreMer}, Kit^{MerCreMer} and Cx3cr1^{CreERT2}, where the inducible Cre is inserted-in the endogenous locus. For both Runx1^{MerCreMer} and Kit^{MerCreMer}, developmental hematopoietic defects have been described in heterozygous embryos. Collectively, the method presented here allows to investigate yolk sac EMP biology during development and also yolk sac-derived macrophages found in adult tissues and distinct from HSC-derived macrophages. This will improve our current understanding of this lineage of resident macrophages and their specific functions in adulthood. The immunophenotypic characterization of EMPs has been improved recently using cell sorting and colony forming assays, demonstrating that yolk sac EMP specifically express CD41 and CD16/32 in early stages of development¹¹. However, the specificity of expression of CD41 and CD16/32 needs further characterization from E10.5 onwards, especially in the fetal liver niche, using fate-mapping models. Indeed, whether CD41 and CD16/32 expression is still specific to EMP when compared to fetal HSCs and HSC-derived progenitors in the E10.5 to E14.5 fetal liver need to be elucidated. The presented method allows to label EMP generated in the yolk sac and to follow them during embryonic development and it will contribute to a more detailed characterization of EMP phenotype when they seed the fetal liver.

This method could be important in the near future to study EMP differentiation pathways. While EMPs emerge from the yolk sac endothelium from E8.5 to E10.5⁴, this method only allows to label a fraction of the progenitors emerging between E8.5-E9.5. Therefore, a limitation of this method is that only a small fraction of EMP is labeled, thus rendering difficult the analysis in classical loss-of-function studies with floxed alleles for candidate genes. Alternatively, sparse labeling could become an advantage in clonal studies of EMP differentiation *in vivo*, using clonal reporter. Nevertheless, the labeling efficiency needs to be characterized for each floxed reporter or floxed allele used, as recombination efficiency of floxed constructs depends on genomic locus (floxed alleles) or the Rosa26 reporter construct. Indeed, different Rosa26 reporter lines are available with different promoters and it is reported that Rosa26^{tdTomato} and Rosa26^{mtmG} strain have higher recombination efficiency than the Rosa26^{LSL-eYFP} line. The reporter mouse strain used in this protocol is Rosa26^{LSL-eYFP} line, which cannot provide information regarding the dynamic process of progenitor maturation mentioned in the results section. The question of maturation process can be partially addressed using different reporter strains like the Rosa26^{mtmG}. In such strain, cells can be distinguished based on the time elapsed since the recombination event. All cells in the Rosa26^{mtmG} strain express membrane-bound tdTomato fluorescent protein and Cre recombination excises the tdTomato cassette and allows for expression of membrane-bound GFP. Since tdTomato has a long half-life, cells that still contain tdTomato but have started to express the GFP (shortly after recombination) are tdTomato⁺ GFP^{low/int} and can be distinguished from tdTomato^{neg} GFP⁺ cells that do not express tdTomato anymore and express higher levels of GFP (later after recombination).

As discussed above, OH-TAM preparation is a critical step to consistently deliver similar doses of OH-TAM between experiments and to reduce tamoxifen side effects. Progesterone co-administration is also useful to limit deleterious effect of tamoxifen on pregnancy. Another critical element of the protocol is the viability of the single-cell suspension obtained from different embryonic tissues. We usually obtain >90% viable cells for flow cytometric analysis. To achieve this, it is critical to follow all the steps rapidly and to maintain all samples on ice after tissue

collection. Appropriate controls such as unstained samples, single stains and fluorescent minus one (FMO) controls are required to identify gate boundaries and to control for the spectral overlap in multicolor panels. Changes in the antibody need to be validated in terms of antibody titration and spectral overlap. Finally, the choice of the Rosa26 reporter strain needs to be adapted to the scientific question that is investigated.

Disclosures

The authors have nothing to disclose.

Acknowledgements

The authors thank Prof Frederic Geissmann and Prof Christian Schulz for insightful discussions; Dr Hannah Garner for critical reading of the manuscript, Dr Xavier Montagutelli and Dr Jean Jaubert and the staff of the Institut Pasteur animal facility for support with mouse husbandry; and Pascal Dardenne and Vytaute Boreikaite, an Amgen Scholar, for their technical assistance. Research in the E.G.P. laboratory is funded by the Institut Pasteur, the CNRS, the Cercle FSER (FRM) and a starting package from the Institut Pasteur and the REVIVE consortium. L.I. is supported by a PhD fellowship from the REVIVE consortium.

References

- Bertrand, J. Y. *et al.* Three pathways to mature macrophages in the early mouse yolk sac. *Blood*. **106** (9), 3004-3011 (2005).
- Palis, J., Robertson, S., Kennedy, M., Wall, C., & Keller, G. Development of erythroid and myeloid progenitors in the yolk sac and embryo proper of the mouse. *Development*. **126** (22), 5073-5084 (1999).
- Chen, M. J. *et al.* Erythroid/myeloid progenitors and hematopoietic stem cells originate from distinct populations of endothelial cells. *Cell Stem Cell*. **9** (6), 541-552 (2011).
- Frame, J. M., Fegan, K. H., Conway, S. J., McGrath, K. E., & Palis, J. Definitive Hematopoiesis in the Yolk Sac Emerges from Wnt-Responsive Hemogenic Endothelium Independently of Circulation and Arterial Identity. *Stem Cells*. (2015).
- Kiusesseian, A., Brunet de la Grange, P., Burlen-Defranoux, O., Godin, I., & Cumano, A. Immature hematopoietic stem cells undergo maturation in the fetal liver. *Development*. **139** (19), 3521-3530 (2012).
- Gomez Perdiguero, E. *et al.* Tissue-resident macrophages originate from yolk-sac-derived erythro-myeloid progenitors. *Nature*. **518** (7540), 547-551 (2015).
- Hoefel, G. *et al.* C-Myb(+) erythro-myeloid progenitor-derived fetal monocytes give rise to adult tissue-resident macrophages. *Immunity*. **42** (4), 665-678 (2015).
- Kierdorf, K., Prinz, M., Geissmann, F., & Gomez Perdiguero, E. Development and function of tissue resident macrophages in mice. *Semin Immunol*. **27** (6), 369-378 (2015).
- Houssaint, E. Differentiation of the mouse hepatic primordium. II. Extrinsic origin of the haemopoietic cell line. *Cell Differ*. **10** (5), 243-252 (1981).
- Cumano, A., & Godin, I. Ontogeny of the hematopoietic system. *Annu Rev Immunol*. **25** 745-785 (2007).
- McGrath, K. E. *et al.* Distinct Sources of Hematopoietic Progenitors Emerge before HSCs and Provide Functional Blood Cells in the Mammalian Embryo. *Cell Rep*. **11** (12), 1892-1904 (2015).
- Schulz, C. *et al.* A lineage of myeloid cells independent of Myb and hematopoietic stem cells. *Science*. **336** (6077), 86-90 (2012).
- Chevalier, C., Nicolas, J. F., & Petit, A. C. Preparation and delivery of 4-hydroxy-tamoxifen for clonal and polyclonal labeling of cells of the surface ectoderm, skin, and hair follicle. *Methods Mol Biol*. **1195** 239-245 (2014).
- Bertrand, J. Y., Giroux, S., Cumano, A., & Godin, I. Hematopoietic stem cell development during mouse embryogenesis. *Methods Mol Med*. **105** 273-288 (2005).
- Bertrand, J. Y. *et al.* Characterization of purified intraembryonic hematopoietic stem cells as a tool to define their site of origin. *Proc Natl Acad Sci U S A*. **102** (1), 134-139 (2005).
- Ginhoux, F. *et al.* Fate mapping analysis reveals that adult microglia derive from primitive macrophages. *Science*. **330** (6005), 841-845 (2010).
- Nakamura, E., Nguyen, M. T., & Mackem, S. Kinetics of tamoxifen-regulated Cre activity in mice using a cartilage-specific CreER(T) to assay temporal activity windows along the proximodistal limb skeleton. *Dev Dyn*. **235** (9), 2603-2612 (2006).
- Qian, B. Z. *et al.* CCL2 recruits inflammatory monocytes to facilitate breast-tumour metastasis. *Nature*. **475** (7355), 222-225 (2011).
- Yona, S. *et al.* Fate mapping reveals origins and dynamics of monocytes and tissue macrophages under homeostasis. *Immunity*. **38** (1), 79-91 (2013).
- Sheng, J., Ruedl, C., & Karjalainen, K. Most Tissue-Resident Macrophages Except Microglia Are Derived from Fetal Hematopoietic Stem Cells. *Immunity*. **43** (2), 382-393 (2015).